JOURNAL OF EXPERIMENTAL NANOSCIENCE
2021, VOL. 16, NO. 1, 369–382
https://doi.org/10.1080/17458080.2021.1975037

Green synthesis of nickel nanoparticles using *Fumaria officinalis* as a novel chemotherapeutic drug for the treatment of ovarian cancer

Yan Huang[a]*, Chunxia Zhu[b]*, Rongkai Xie[a] and Ming Ni[c]

[a]Department of Obstetrics and Gynecology, Chongqing Xinqiao Hospital, Second Affiliated Hospital of Army Medical University, Chongqing, China; [b]Dapartment of Gynecology, Xianning Central Hospital (The first Affiliated Hospital of Hubei University of Science and Technology), Xianning, Hubei, China; [c]Department of Obstetrics and Gynecology, Wuhan Hanyang hospital, Wuhan, China

ABSTRACT

In the present study, nickel nanoparticles were green-synthesized using the aqueous extract of *Fumaria officinalis*. The synthesized NiNPs@*F. officinalis* were characterized by analytical techniques including EDX, FE-SEM, XRD, UV-Vis., and FT-IR. The antioxidant and anti-ovarian cancer activity of NiNPs@*F. officinalis* was evaluated. The nanoparticles were formed in a spherical shape in the range of 16.85 to 49.04 nm for the particle size. In the antioxidant test, the IC_{50} of *F. officinalis*, NiNPs@*F. officinalis*, and BHT against DPPH free radicals were 253, 145, and 107 μg/mL, respectively. In the cellular and molecular part of the recent study, the treated cells with NiNPs@*F. officinalis* were assessed by MTT assay for 48 h about the cytotoxicity and anti-human ovarian cancer properties on normal (HUVEC) and ovarian cancer cell lines i.e. PA-1, Caov-3, SW-626, and SK-OV-3. The viability of malignant ovarian cell line reduced dose-dependently in the presence of NiNPs@*F. officinalis*. The IC_{50} of NiNPs@*F. officinalis* were 375, 225, 246, and 279 μg/mL against PA-1, Caov-3, SW-626, and SK-OV-3 cell lines, respectively. After the clinical study, nickel nanoparticles containing *F. officinalis* leaf aqueous extract may be used to formulate a new chemotherapeutic drug or supplement to treat several types of human ovarian cancer.

ARTICLE HISTORY
Received 9 August 2021
Accepted 24 August 2021

KEYWORDS
Green synthesis; chemical characterization; nickel nanoparticles; anti-ovarian cancer; antioxidant

1. Introduction

The previous studies have been indicating when metallic nanoparticles are green-synthesized by ethnomedicinal plants rich in antioxidant molecules, their therapeutic properties such as anti-human cancer effects significantly increase. A great number of doctors use chemotherapy, immunotherapy, and radiation therapy to treat several types of cancers [1–3]. Chemotherapeutic drugs have a bad effect on the body, so today the formulation of an effective chemotherapy drug from metallic nanoparticles is important [2, 3].

CONTACT Ming Ni niming202122@sina.com Department of Obstetrics and Gynecology, Wuhan Hanyang hospital, Wuhan, China
*Yan Huang and Chunxia Zhu contributed equally to the article.

Nanotechnology is the field to yield modern systems, tools, and materials by taking control at the atomic and molecular levels using the features that appear on those surfaces. Applications for nanotechnology in medical diagnostics, food, medicine, biotechnology, environment, energy, chemistry, physics, etc, introduce this technology as an interdisciplinary and cross-sectoral context. The interdisciplinary nature of nanoscience and nanotechnology as the field to yield modern systems, tools, and materials with precision atoms and molecules, will sooner or later affect the health and medical sector [1–4].

Drug use is currently volumetric, so most cells in the body need medication. In the new method, the drug is directed directly to specific cells with new injection devices and delivered to the required location. By this mechanism, small and large diseases can be diagnosed and treated at the beginning of their formation [1, 2]. The National Nanotechnology Project is being implemented in European countries, the United States, and Japan with high priority in various fields. Nanotechnology and nanoscience emerging fields can move materials very accurately, to understand and control unprecedented fundamental components of physical objects. It seems that these developments will change the way we design and build everything from vaccines to computers. The plan would increase investment in nanotechnology by about twice as much each year as last year. A branch of nanotechnology is the formulation of new drugs with metal nanoparticles [1–3]. Today, nanoparticles have become very popular due to their wide applications in biology, medicine, and medicine. Structurally, their size is in the range of 100 nanometers. Several drugs such as small hydrophobic and hydrophilic drugs, molecules, and vaccines of biological nanoparticles can be administered by these nanoparticles. They are widely used in improving the treatment and diagnosis of diseases. Nanoparticles in nanoliposomes, carbon nanotubes, nanofibers, nanospheres have been widely used for drug carriers and in the manufacture of cell scaffolds [2, 5].

Applications of nanoparticles in drug delivery include drug carriers in diseases such as cancer, cardiovascular disease, and Alzheimer's. The use of these nanocarriers is very effective for neurological diseases such as Alzheimer's. Due to their size, these nanoparticles can cross the blood-brain barrier, which has always been a barrier to the passage of drugs to the affected area in this type of destructive brain disease. Due to their small size, nanoparticles can also be used in brain cancers [3]. The goal in making nanoparticles is to control the surface properties, particle size, and release of a specific and efficient drug in a specific place and time for the drug to be as effective as possible. Nanoparticles are widely used in tissue engineering scaffolds, targeted drug delivery, and disease diagnosis. At present, many drug delivery systems are made of nanoparticles and different materials have been used as drug stimulants or enhancers to ameliorate the effectiveness of treatment and the durability and stability as well as the safety of anticancer drugs [1, 2]. The substances used to release cancer drugs are divided into different polymers, magnetic, and biomolecules. These materials can also provide surface modifications such as binding to target antibodies and ligands to make the nanoparticles act purposefully to increase the effectiveness of the treatment [2].

In recent years, research on applications of metallic nanoparticles is one of the interesting filed around the world. The particle size, distribution, architecture, chemical assembly, colloidal stability, and biocompatibility are the most important factors that affect the metallic nanoparticles applications [6, 7]. Metallic nanoparticles containing medicinal plants have very significant anti-cancer effects. In recent years, these metal nanoparticles containing herbs have been used to treat various cancers of the ovaries, prostate, esophagus, stomach, lungs, and various leukemias [1–3, 8–10].

One of the most important cancers in recent years is ovarian cancer. Many medicinal plants including *Allium sativum*, *Zingiber officinale*, *Camellia sinensis*, *Ginkgo biloba*, *Quercus tinctoria*, *Camptotheca acuminate*, *Podophyllum peltatum*, *Taxus brevifolia*, *Azadirachta indica*, *Asparagus racemosus*, *Symplocus racemosa*, *Saraca indica*, and *Curcuma longa* are used in traditional medicine to treat ovarian cancer [9]. It is predicted that if metal nanoparticles are synthesized and formulated with these plants, their anticancer effects against ovarian cancer cells will be much stronger.

Fumitory or *Fumaria officinalis* is the famous species of Fumariaceae family. The plant is known as a popular plant in various traditional medicines around the world. The plant grows in many regions such as Europe, Asia, and Africa [11, 12]. Different medicinal uses have been reported for *F. officinalis* in Bulgarian traditional medicine is used as antihypertensive, diuretic, hepatoprotectant, and for treatment of skin rashes [13]. in many countries, the plant is used to treat skin diseases, rheumatism, or hypertension. In many African countries, the plant is used in hypertension, constipation, liver detoxification, and spasmolytic. In Iranian traditional medicine, the plant is also used in skin diseases, scabies, antiscorbite, anti-bronchitis [14]. *F. officinalis* is rich in isoquinoline alkaloids and flavone heterosides [15, 16]. Protopine, aporphine, benzophenanthridine, and protoberberine are the important alkaloids in *F. officinalis* [17]. In the current research, nickel nanoparticles are green-synthesized using *F. officinalis* leaf aqueous extract. The synthetic nanoparticles were characterized by different analytical techniques. The biological activity of the nanoparticles such as antioxidant, cytotoxicity, and anticancer activity against common ovarian cancer cell lines i.e. PA-1, Caov-3, SW-626, and SK-OV-3 were evaluated.

2. Material and methods

2.1. Preparation and extraction of aqueous extract

First, the dried leaves of *F. officinalis* were grounded. Then, 100 g of the sample was macerated in 750 mL of boiling water for 3 h. After filtration, the extract was placed in a rotary evaporator (Buchi) to concentrate the crude extract. Finally, the extract was put in a freeze drier for 72 h to produce the powder extract of *F. officinalis*.

2.2. Green synthesis and chemical characterization of NiNPs@F. officinalis

A reported procedure (with some modifications) was used to green-synthesis of NiNPs@*F. officinalis* [18]. First, 10 mL of the plant extract (2 g in 20 mL of water) was added to 30 mL of 15 mM $NiSO_4$. $6H_2O$. Then, one mL of NaOH (2%) was added dropwise and shake for 20 min. The container was placed in an ultrasonic bath (75 W) for 25 min. After the time, a green nickel nanoparticle was formed. The obtained NiNPs@*F. officinalis* was washed three times with water and centrifuged at 12000 rpm for 10 min. Finally, the precipitate was dried in an oven at 50 °C.

2.3. Antioxidant activities of NiNPs@F. officinalis

The free radical scavenging test was first performed by Blois in 1958, and after some modification by numerous studies in its current form. DPPH method is one of the most widely used methods for estimating antioxidant content. DPPH is a stable radical that reacts with hydrogen atom compounds. This test is based on the inhibition of DPPH, which causes the decolorization of DPPH solution by adding radical species or

antioxidants. DPPH changes color from purple to yellow by taking an electron from the antioxidant compound. The free radicals in DPPH are adsorbed at 517 nm, which follows Beer Lambert's law, and decreased absorption is linearly related to the amount of antioxidants; the higher the amount of antioxidants, the more DPPH is consumed and the more purple turns yellow [19].

The degree of inhibition of DPPH radicals was evaluated by Shaneza *et al.* (2018) [19]. For this purpose, solutions with different samples of the $NiSO_4$, *F. officinalis* leaf aqueous extract and NiNPs@*F. officinalis* of variable concentrations (0-1000 µg/mL) as well as synthetic antioxidant BHT in methanol solvent were prepared. The test method was that one mLo f DPPH methanolic solution (at a concentration of 1 mM) was added to 4 mL of the extract and the resulting mixture was stirred vigorously. The test tubes were placed in a dark place for 60 min. After this period, the absorbance was read at 517 nm. Finally, the DPPH radicals' inhibition percentage of the $NiSO_4$, *F. officinalis* leaf aqueous extract, and NiNPs@*F. officinalis* was calculated by the below formula [19]:

$$\text{Inhibition } (\%) = \frac{Sample\ A.}{Control\ A.} x100$$

IC_{50} factor was used to evaluate better the antioxidant activity, which indicates the concentration of the $NiSO_4$, *F. officinalis* leaf aqueous extract, and NiNPs@*F. officinalis* that can reduce the concentration of free radical DPPH. The initial is 50% of the initial value, and the lower the amount, the greater the antioxidant activity [19].

2.4. Anti-human ovarian cancer properties of NiNPs@F. officinalis

MTT is a colorimetric technique. Based on the fact that living cells can do oxidative metabolism, as a result, oxidation, breaks down the MTT dye and produces a dye ranging from yellow to blue. This test determines the number of living cells [20].

In this research, we used the following Cell lines to evaluating anti-human ovarian cancer and cytotoxicity effects of $NiSO_4$, *F. officinalis* leaf aqueous extract, and NiNPs@*F. officinalis* using an MTT method.

I. Human ovarian cancer cell lines: PA-1, Caov-3, SW-626, and SK-OV-3.
II. Normal cell line: HUVEC.

These cell lines were cultured in appropriate numbers (10,000 cells/well) in a 96-well microplate. They were then incubated at 37° C and 5% CO2 for 24 h to form a cell monolayer. Then, out of the greenhouse and under the hood, different concentrations of $NiSO_4$, *F. officinalis* leaf aqueous extract, and NiNPs@*F. officinalis* were added to the cells. Control wells also included cell control containing complete cell and culture medium and blank control containing no cell and complete culture medium, and the microplates were again placed in the oven at 37° C and 5% CO2 until the required time (24-48-72 h). After the test times, the cells were washed with PBS saline phosphate, MTT dye was added to the wells and the microplates were incubated for 3 h. Finally, the optical absorption of cells at 570 nm was read by the ELISA reader (model: Tek Bio Elx800). The cell viability percentage was calculated by the following formula [20]:

$$\text{Cell viability } (\%) = \frac{Sample\ A.}{Control\ A.} x100$$

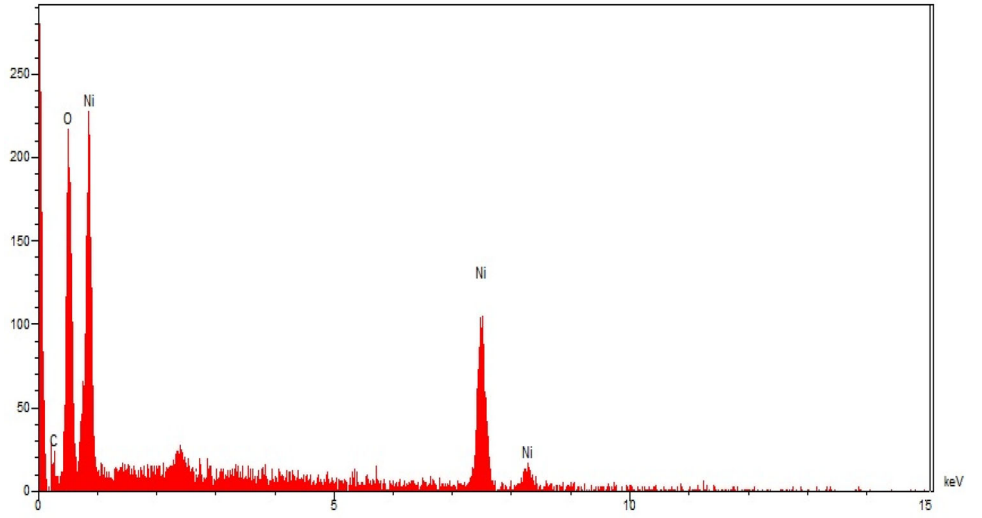

Figure 1. EDX analysis of NiNPs@F. *officinalis*.

2.5. Qualitative measurement

After collecting data, Minitab statistical software was used for statistical analysis. Evaluation of antioxidant results in a completely randomized design and comparison of means was Duncan's pos-thoc test with a maximum error of 5%. To measure the percentage of cell survival in factorial experiments with the original design of completely randomized blocks and compare the means, the Duncan post-hoc test with a maximum error of 5% was used. The 50% cytotoxicity (IC_{50}) and 50% free radical scavenging (IC_{50}) was estimated with ED_{50} plus software (INER, V: 1.0). Measurements were reported as mean ± standard deviation.

3. Results and discussion

3.1. Chemical characterization of NiNPs@F. officinalis

EDX analysis: The qualitative analysis of EDX was run to screen the elemental analysis of NiNPs@*F. officinalis*. The EDX diagram of NiNPs is shown in Figure 1. The findings approved the appearance of nickel (by the peaks at 0.85 keV for NiLα, 7.5 keV for NiKα, and 8.2 keV for NiKβ), oxygen (by the peak at 0.51 keV for OLα), and carbon (by the peak at 0.22 keV for CLα) in NiNPs@*F. officinalis*. The signal for nickel has been reported by other research groups [21]. The presence of oxygen and carbon approved the linkage between nickel nanoparticles and organic compounds of the plant extract. Besides, the Ni nanoparticles may be formed as NiO formula.

SEM analysis: The morphology of NiNPs@*F. officinalis* was assessed by the FE-SEM technique. Figure 2 shows the FE-SEM of NiNPs@*F. officinalis*. The images show the spherical shape for the nanoparticles with particle size in the range of 16.85 to 49.04 nm. Furthermore, the nanoparticles are aggregated. This is a general property of the biosynthesized metallic nanoparticles, that was found in our literature review [3, 22–24]. In our review of literature, the size of nickel nanoparticles, which were synthesized using plant extract was in the range of 18 to 72 nm [25–29].

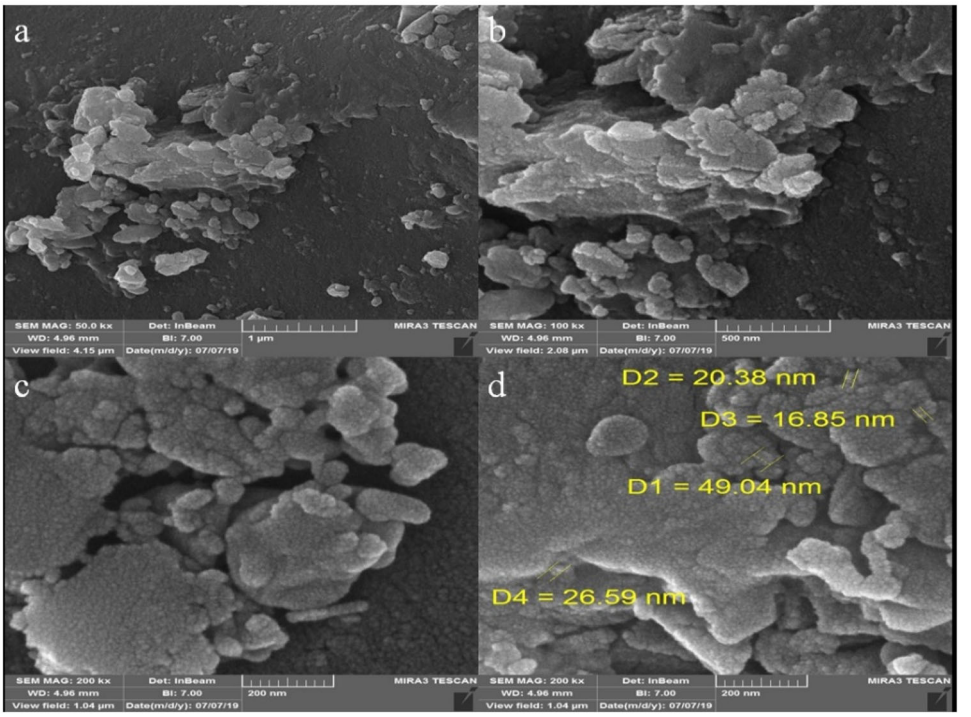

Figure 2. FE-SEM images of NiNPs@*F. officinalis*.

XRD analysis: The XRD diffraction patterns of NiNPs@*F. officinalis* evaluated its crystallinity. The pattern of the diffractogram is showed in Figure 3. The formation of nanoparticles was approved to this result. Despite the small size of NiNPs@*F. officinalis*, the pattern of XRD indicated well crystallizing. The achieved data were compared with the standard database of JCPDS card no. 1313-991. The signals with 2θ values of 26.92, 37.35, 43.28, 62.87, and 75.98 are indexed as (110), (111), (200), (220), and (311) planes. A 16.91 nm was measured for the crystal size of NiNPs@*F. officinalis* that was calculated using X-ray diffraction and according to Scherer's equation. According to previous studies, the crystal size of green synthesized nickel nanoparticles was in the range of 8 to 43.9 nm [25, 30–32].

FT-IR analysis: The FT-IR spectra of nickel nanoparticles and *F. officinalis* are shown in Figure 4. The formation of NiNPs@*F. officinalis* is approved by the presence of the peaks at wavenumbers of 433, 534, and 603 cm^{-1} that belong to the vibration of Ni-O. Similar peaks with some differences in the wavenumber have been reported for green-synthetic NiNPs by other research groups. A similarity is observed in the spectra of the nanoparticles and *F. officinalis* extract. The peaks in the NPs spectrum are attributed to the functional groups of different organic compounds in *F. officinalis* extract, which are linked to the surface of NiNPs@*F. officinalis*. The presence of secondary metabolites such as alkaloids, carbohydrates, phenolic compounds, flavonoids, glycosides, and terpenoids in *F. officinalis* extract have been reported previously [14, 15, 33]. The peaks in 3404 and 2927 cm^{-1} are related to O-H and aliphatic C-H stretching; the peaks from 1431 to 1675 cm^{-1} are corresponded to C = C and C = O stretching, and the peaks at 1261 and 1085 cm^{-1} could be ascribed to -C-O and C-N stretching.

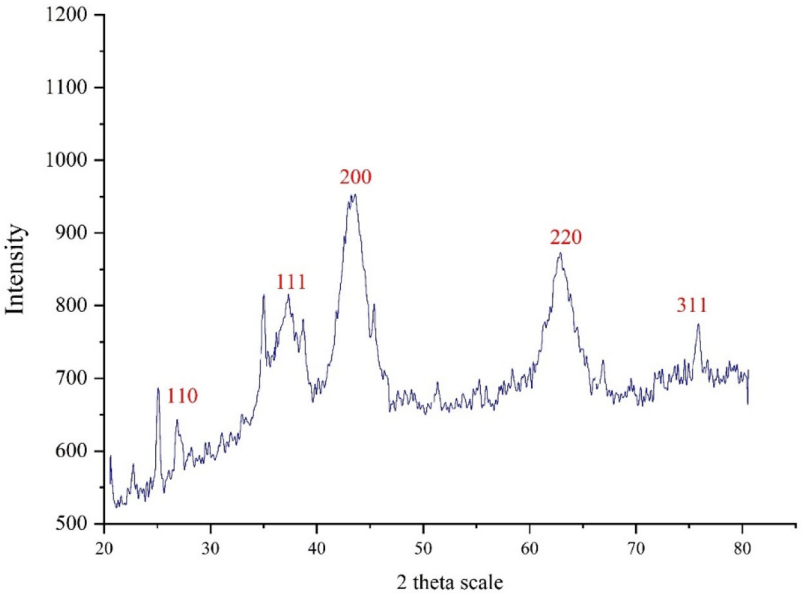

Figure 3. XRD Pattern of NiNPs@*F. officinalis*.

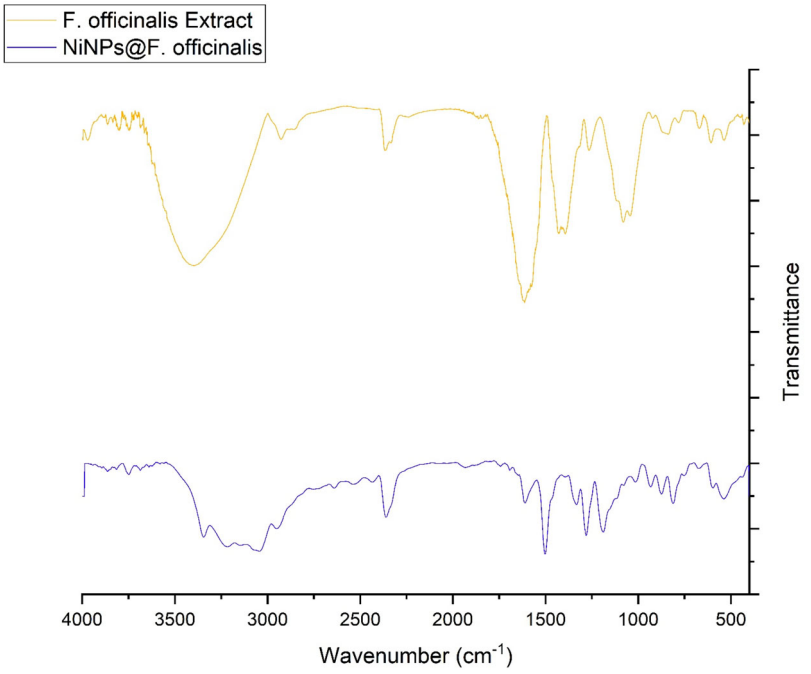

Figure 4. FT-IR Spectra of NiNPs@*F. officinalis* and *F. officinalis* extract.

UV-Vis. analysis: The UV–Vis. spectrum of the green-synthetic nanoparticles of NiNPs@*F. officinalis* is presented in Figure 5. The surface plasmon resonance (SPR) of NiNPs@*F. officinalis* was completed using UV–Vis. spectroscopy. The creation of the bio-synthetic NiNPs@*F. officinalis* was observed. There was an advanced SPR band appearance at the wavelength range of 341 nm that approved the formation of the nanoparticles.

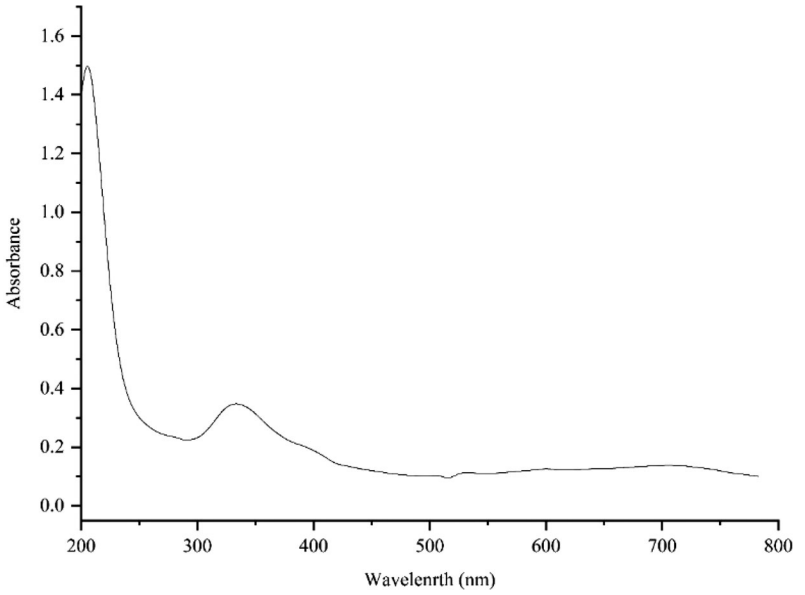

Figure 5. UV–Vis. spectrum of NiNPs@*F. officinalis*.

The band is very close to a previously reported on the green synthesized of nickel nanoparticles using *Calendula officinalis* extract [21].

3.2. Cytotoxicity and anti-human ovarian cancer activities of NiNPs@F. officinalis

One of the cytotoxicity test methods to measure the rate of cell death is the MTT method, which is based on the formation of formazan dye by reducing the substance MTT (dimethyl thiazole 2 and 5 diphenyltetrazolium bromide) or other tetrazolium salts [34–36]. By breaking the MTT tetrazolium ring by mitochondrial enzymes in living cells, insoluble purple formazan crystals are formed. The formation of these crystals indicates the activity of respiratory chain enzymes and is a measure of cell viability. By measuring the amount of absorption by spectrophotometer at specific wavelengths, the number of living cells can be determined. This test is performed according to ISO 10993-5 and its purpose is *in vitro* evaluation of cytotoxicity. Cytotoxicity test is performed according to ISO10993-5 standard and in three ways: NRU test, CFU test, MTT test, and XTT test. The most common method for assessing cytotoxicity is to measure cell survival by MTT [35–37].

The basis of the MTT method is based on the intensity of dye produced by the mitochondrial activity of cells, that measured at a wavelength of 540 to 630 nm and directly proportional to the number of living cells, the increase or decrease in the number of living cells is linearly related to the activity of cell mitochondria. MTT tetrazolium dye is revived in the active cells (metabolically). Mitochondrial dehydrogenases in living cells produce NADH and NADPH, leading to an insoluble purple precipitate called formazan. This precipitate can be dissolved by isopropanol or dimethyl sulfoxide [35–38]. Dead cells, on the other hand, are unable to perform this conversion due to the inactivity of their mitochondria and therefore do not show a signal. In this method, dye formation is used as a marker for the presence of living cells [38, 39]. In recent years, MTT testing has

Table 1. The anti-human ovarian cancer properties of $NiSO_4$, *F. officinalis*, and NiNPs@*F. officinalis* against human breast carcinoma cell lines.

	Cell *via*bility (%)				
Concentration (μg/mL)	HUVEC	PA-1	Caov-3	SW-626	SK-OV-3
$NiSO_4$ (0)	100 ± 0^{a}	100 ± 0^{a}	100 ± 0^{a}	100 ± 0^{a}	100 ± 0^{a}
$NiSO_4$ (1)	100 ± 0^{a}	100 ± 0^{a}	100 ± 0^{a}	100 ± 0^{a}	100 ± 0^{a}
$NiSO_4$ (2)	100 ± 0^{a}	100 ± 0^{a}	100 ± 0^{a}	100 ± 0^{a}	100 ± 0^{a}
$NiSO_4$ (3)	100 ± 0^{a}	100 ± 0^{a}	100 ± 0^{a}	100 ± 0^{a}	100 ± 0^{a}
$NiSO_4$ (7)	100 ± 0^{a}	100 ± 0^{a}	100 ± 0^{a}	100 ± 0^{a}	100 ± 0^{a}
NiSO4 (15)	98.2 ± 1.3^{a}	100 ± 0^{a}	100 ± 0^{a}	100 ± 0^{a}	100 ± 0^{a}
$NiSO_4$ (31)	94 ± 0.7^{a}	99.2 ± 0.44^{a}	100 ± 0^{a}	100 ± 0^{a}	100 ± 0^{a}
$NiSO_4$ (62)	88.6 ± 0.89^{a}	96 ± 0.7^{a}	98 ± 1^{a}	99.6 ± 1.14^{a}	98 ± 0.7^{a}
$NiSO_4$ (125)	83 ± 1^{a}	91 ± 0.7^{a}	94.6 ± 0.89^{a}	92.2 ± 1.3^{a}	94.2 ± 0.83^{a}
$NiSO_4$ (250)	77.6 ± 1.14^{ab}	86 ± 1^{a}	89.6 ± 0.89^{a}	84 ± 1.22^{a}	87 ± 1^{a}
$NiSO_4$ (500)	70 ± 1.22^{ab}	79.2 ± 0.44^{ab}	83.2 ± 0.83^{a}	78.2 ± 0.83^{ab}	79.6 ± 1.14^{ab}
$NiSO_4$ (1000)	62.6 ± 1.14^{ab}	73 ± 0.7^{ab}	75 ± 1.22^{ab}	69 ± 1^{ab}	68.2 ± 0.44^{ab}
F. officinalis (0)	100 ± 0^{a}	100 ± 0^{a}	100 ± 0^{a}	100 ± 0^{a}	100 ± 0^{a}
F. officinalis (1)	100 ± 0^{a}	100 ± 0^{a}	100 ± 0^{a}	100 ± 0^{a}	100 ± 0^{a}
F. officinalis (2)	100 ± 0^{a}	100 ± 0^{a}	100 ± 0^{a}	100 ± 0^{a}	100 ± 0^{a}
F. officinalis (3)	100 ± 0^{a}	100 ± 0^{a}	100 ± 0^{a}	100 ± 0^{a}	100 ± 0^{a}
F. officinalis (7)	100 ± 0^{a}	100 ± 0^{a}	100 ± 0^{a}	100 ± 0^{a}	100 ± 0^{a}
F. officinalis (15)	100 ± 0^{a}	98.4 ± 0.54^{a}	98.6 ± 0.89^{a}	99 ± 0.7^{a}	98.4 ± 0.54^{a}
F. officinalis (31)	100 ± 0^{a}	96.2 ± 0.83^{a}	94.6 ± 1.14^{a}	95 ± 1^{a}	96.4 ± 0.89^{a}
F. officinalis (62)	99.4 ± 0.54^{a}	91.6 ± 1.14^{a}	88.2 ± 1.3^{a}	89.2 ± 0.83^{a}	88 ± 1^{a}
F. officinalis (125)	97.4 ± 0.89^{a}	83 ± 0.7^{a}	76.4 ± 0.89^{ab}	79 ± 0.7^{ab}	80.6 ± 1.14^{ab}
F. officinalis (250)	94.2 ± 1.3^{a}	72.6 ± 0.89^{ab}	62 ± 0.7^{ab}	65.4 ± 0.54^{ab}	67.2 ± 0.83^{ab}
F. officinalis (500)	91 ± 1.22^{a}	57 ± 1.22^{b}	49.6 ± 1.14^{b}	50 ± 1^{b}	51 ± 1.22^{b}
F. officinalis (1000)	87.6 ± 0.89^{a}	34.4 ± 0.54^{bc}	23.4 ± 0.89^{bc}	30.6 ± 0.89^{bc}	26.2 ± 0.83^{bc}
NiNPs@*F. officinalis* (0)	100 ± 0^{a}	100 ± 0^{a}	100 ± 0^{a}	100 ± 0^{a}	100 ± 0^{a}
NiNPs@*F. officinalis* (1)	100 ± 0^{a}	100 ± 0^{a}	100 ± 0^{a}	100 ± 0^{a}	100 ± 0^{a}
NiNPs@*F. officinalis* (2)	100 ± 0^{a}	100 ± 0^{a}	100 ± 0^{a}	100 ± 0^{a}	100 ± 0^{a}
NiNPs@*F. officinalis* (3)	100 ± 0^{a}	100 ± 0^{a}	100 ± 0^{a}	100 ± 0^{a}	99 ± 1^{a}
NiNPs@*F. officinalis* (7)	100 ± 0^{a}	99.2 ± 0.44^{a}	99.4 ± 0.54^{a}	99.4 ± 0.54^{a}	96.4 ± 0.89^{a}
NiNPs@*F. officinalis* (15)	100 ± 0^{a}	96 ± 0.7^{a}	94.2 ± 1.3^{a}	96.2 ± 0.83^{a}	90.2 ± 0.83^{a}
NiNPs@*F. officinalis* (31)	99.4 ± 0.54^{a}	90.6 ± 1.14^{a}	87.6 ± 0.89^{a}	89 ± 1^{a}	83 ± 1.22^{a}
NiNPs@*F. officinalis* (62)	98.6 ± 0.89^{a}	84.6 ± 1.14^{a}	76.2 ± 0.83^{ab}	78.2 ± 0.44^{ab}	76 ± 0.7^{ab}
NiNPs@*F. officinalis* (125)	94 ± 1^{a}	74.2 ± 0.83^{ab}	62 ± 1.22^{ab}	64.2 ± 0.83^{ab}	66.2 ± 1.3^{ab}
NiNPs@*F. officinalis* (250)	89.4 ± 0.89^{a}	60 ± 1.22^{b}	47 ± 0.7^{b}	49.4 ± 0.54^{b}	52 ± 1^{b}
NiNPs@*F. officinalis* (500)	83 ± 1.22^{a}	40 ± 1^{bc}	29.2 ± 1.3^{bc}	32 ± 1^{bc}	35.6 ± 0.89^{bc}
NiNPs@*F. officinalis* (1000)	75.2 ± 0.44^{ab}	13.4 ± 0.89^{c}	4.6 ± 0.89^{c}	8.6 ± 0.89^{c}	9.6 ± 1.14^{c}

The several words present significant differences between experimented groups ($p \leq 0.01$).

been the most important measurement method to evaluate the toxicity and anti-cancer effects of metal nanoparticles [20, 38, 39].

In this investigation, the treated cells with different concentrations of the present $NiSO_4$, *F. officinalis* leaf aqueous extract, and NiNPs@*F. officinalis* were assessed by MTT assay for 48 h about the cytotoxicity properties on normal (HUVEC) and ovarian malignancy cell lines i.e. PA-1, Caov-3, SW-626, and SK-OV-3. The absorbance rate was evaluated at 570 nm, which represented viability on normal cell line (HUVEC) even up to 1000 μg/mL for $NiSO_4$, *F. officinalis* leaf aqueous extract, and NiNPs@*F. officinalis* (Tables 1 and 2).

The viability of malignant ovarian cell line reduced dose-dependently in the presence of $NiSO_4$, *F. officinalis* leaf aqueous extract, and NiNPs@*F. officinalis*. The IC_{50} of NiNPs@*F. officinalis* were 375, 225, 246, and 279 μg/mL against PA-1, Caov-3, SW-626, and SK-OV-3 cell lines, respectively (Tables 1 and 2). The IC_{50} of *F. officinalis* leaf aqueous extract were 652, 497, 500, and 520 μg/mL against PA-1, Caov-3, SW-626, and SK-OV-3 cell lines, respectively (Tables 1 and 2).

Table 2. The IC_{50} of $NiSO_4$, *F. officinalis*, and NiNPs@*F. officinalis* in cytotoxicity and anti-ovarian cancer tests.

	$NiSO_4$ (μg/mL)	*F.officinalis* (μg/mL)	NiNPs@*F. officinalis* (μg/mL)
IC_{50} against HUVEC	–	–	–
IC_{50} against PA-1	–	652 ± 0^a	375 ± 0^c
IC_{50} against Caov-3	–	497 ± 0^b	225 ± 0^d
IC_{50} against SW-626	–	500 ± 0^b	246 ± 0^d
IC_{50} against SK-OV-3	–	520 ± 0^b	279 ± 0^d

The several words present significant differences between experimented groups ($p \leq 0.01$).

3.3. Antioxidant properties of NiNPs@F. officinalis

In this study, we assessed the antioxidant properties of *F. officinalis* leaf aqueous extract green-synthesized NiNPs@*F. officinalis* by using the DPPH test as a common free radical. Free radicals are atoms, molecules, or ions with unpaired electrons and are therefore very active, unstable, and highly reactive. Free radicals are formed by breaking a bond of a stable molecule. Free radicals collide with other molecules to achieve stability and can separate electrons from them, as a result, they form a chain of more unstable molecules. A free radical can have a positive, negative, or neutral charge [19]. During the body's natural metabolism or under conditions such as smoking, pollution, the entry of unnecessary chemicals into the body in any way, radiation, and stress in the body produce free radicals. The most important free radical in the human body is oxygen, which can damage DNA and other molecules. Oxidative stress is the victory of free radicals over the body's antioxidant defense and is a biological attack on the body [2, 3]. Antioxidants are molecules that can donate an electron to a free radical without destabilizing themselves. This stabilizes the free radical and makes it less reactive. The result of oxidative stress in the body is various degeneration, eye damage, premature aging, muscle problems, brain damage, heart failure, diabetes, cancer, and overall weakness of the immune system [1]. Oxygen radicals are continuously produced in all living organisms and with destructive effects, lead to cell damage and death. The production of oxidant species under physiological conditions has a controlled rate, but this production increases under oxidative conditions [19]. Various studies have shown that antioxidant compounds have very significant anti-cancer effects with omitting the free radicals. Herbs are rich in antioxidant compounds and reduce the risk of some chronic diseases such as cataracts, rheumatoid arthritis, memory loss, stroke, heart disease, and cancer by protecting cells and increasing the power of plasma antioxidants. Flavonoids and alkaloids commonly found in medicinal plants have high antioxidant activity [2, 3].

The scavenging capacity of *F. officinalis* leaf aqueous extract green-synthesized NiNPs@*F. officinalis* and BHT at different concentrations expressed as percentage inhibition has been indicated in Tables 3 and 4. In the antioxidant test, the IC_{50} of *F. officinalis* leaf aqueous extract, NiNPs@*F. officinalis*, and BHT against DPPH free radicals were 253, 145, and 107 μg/mL, respectively (Tables 3 and 4).

It seems that the anti-human ovarian cancer effect of recent nanoparticles is due to their antioxidant effects. Because tumor progression is so closely linked to inflammation and oxidative stress, a compound with anti-inflammatory or antioxidant properties can be an anticarcinogenic agent [40–42]. Many nanoparticles have pharmacological and biochemical properties, including antioxidant and anti-inflammatory properties, which appear to be involved in anticarcinogenic and antimutagenic activities [19, 20]. Today, nanoparticles synthesized by biological methods play a vital role in treating many diseases, including cancer [41, 42]. Nanoparticles synthesized by biological methods are no longer the only ones in traditional medicine, in addition, they have been able to adopt an industrial line of natural products for treating various cancers. Various cell lines from cancers

Table 3. The antioxidant activities of $NiSO_4$, *F. officinalis*, NiNPs@*F. officinalis*, and BHT against DPPH.

Concentration (μg/mL)	DPPH inhibition (%)	Concentration (μg/mL)	DPPH inhibition (%)
BHT (0)	0 ± 0^{a}	*Fumaria officinalis* (0)	0 ± 0^{a}
BHT (1)	0 ± 0^{a}	*Fumaria officinalis* (1)	0 ± 0^{a}
BHT (2)	2 ± 0.7^{a}	*Fumaria officinalis* (2)	1.2 ± 0.44^{a}
BHT (3)	6.4 ± 0.54^{a}	*Fumaria officinalis* (3)	3.4 ± 0.89^{a}
BHT (7)	11.2 ± 0.44^{a}	*Fumaria officinalis* (7)	8.6 ± 0.89^{a}
BHT (15)	18.6 ± 0.89^{ab}	*Fumaria officinalis* (15)	13 ± 1^{a}
BHT (31)	26.2 ± 1.3^{ab}	*Fumaria officinalis* (31)	21.4 ± 0.54^{ab}
BHT (62)	39 ± 1.22^{b}	*Fumaria officinalis* (62)	29.2 ± 0.44^{ab}
BHT (125)	54.6 ± 1.14^{b}	*Fumaria officinalis* (125)	37 ± 1.22^{ab}
BHT (250)	71.6 ± 1.14^{bc}	*Fumaria officinalis* (250)	49.6 ± 0.89^{b}
BHT (500)	92 ± 0.7^{c}	*Fumaria officinalis* (500)	63.2 ± 0.83^{bc}
BHT (1000)	100 ± 0^{c}	*Fumaria officinalis* (1000)	79 ± 1^{c}
Concentration (μg/mL)	**DPPH inhibition (%)**	**Concentration (μg/mL)**	**DPPH inhibition (%)**
NiNPs@*F. officinalis* (0)	0 ± 0^{a}	$NiSO_4$ (0)	0 ± 0^{a}
NiNPs@*F. officinalis* (1)	0 ± 0^{a}	$NiSO_4$ (1)	0 ± 0^{a}
NiNPs@*F. officinalis* (2)	2.4 ± 0.89^{a}	$NiSO_4$ (2)	0 ± 0^{a}
NiNPs@*F. officinalis* (3)	5.4 ± 0.54^{a}	$NiSO_4$ (3)	2.4 ± 0.89^{a}
NiNPs@*F. officinalis* (7)	10 ± 1.22^{a}	$NiSO_4$ (7)	5.2 ± 1.3^{a}
NiNPs@*F. officinalis* (15)	16.2 ± 0.44^{a}	$NiSO_4$ (15)	9 ± 1.22^{a}
NiNPs@*F. officinalis* (31)	23.6 ± 0.89^{ab}	$NiSO_4$ (31)	14 ± 1^{a}
NiNPs@*F. officinalis* (62)	32 ± 0.7^{ab}	$NiSO_4$ (62)	20.2 ± 0.44^{ab}
NiNPs@*F. officinalis* (125)	47.2 ± 1.3^{b}	$NiSO_4$ (125)	26.6 ± 1.14^{ab}
NiNPs@*F. officinalis* (250)	64.4 ± 0.89^{bc}	$NiSO_4$ (250)	33.4 ± 0.89^{ab}
NiNPs@*F. officinalis* (500)	82 ± 1.22^{c}	$NiSO_4$ (500)	38.2 ± 0.44^{b}
NiNPs@*F. officinalis* (1000)	100 ± 0^{c}	$NiSO_4$ (1000)	46.6 ± 0.89^{b}

The different letter present significant differences between experimented groups ($p \leq 0.01$).

Table 4. The IC_{50} of $NiSO_4$, *F. officinalis* leaf aqueous extract, NiNPs@*F. officinalis*, and BHT in the antioxidant test.

Concentration (μg/mL)	BHT	*F.officinalis*	NiNPs@*F. officinalis*	$NiSO_4$
IC_{50} (μg/mL)	107 ± 0^{b}	253 ± 0^{a}	145 ± 0^{b}	–

The different letters present significant differences between experimented groups ($p \leq 0.01$).

of the prostate, ovary, lung, liver, and pancreas have been treated with herbal nanoparticles synthesized [40–42].

4. Conclusion

In conclusion, the green synthesis of nickel nanoparticles was carried out using an aqueous extract of *F. officinalis*. The nanoparticles were characterized using common chemical techniques such as UV-Visible, FT-IR, XRD, FE-SEM, and EDX. The nanoparticles were in a spherical morphology. The size of NiNPs@*F. officinalis* was in the range of 16.85 to 49.04 nm which is well known as a sufficient size for the synthetic nanoparticles. The NiNPs@*F. officinalis* showed the best antioxidant activities against DPPH. The IC_{50} of NiNPs@*F. officinalis* and BHT against DPPH free radicals were 145 and 107 μg/mL, respectively. The viability of malignant ovarian cell line reduced dose-dependently in the presence of NiNPs@*F. officinalis*. The IC_{50} of NiNPs@*F. officinalis* were 375, 225, 246, and 279 μg/mL against PA-1, Caov-3, SW-626, and SK-OV-3 cell lines, respectively. After the clinical study, NiNPs@*F. officinalis* containing *Fumaria officinalis* leaf aqueous extract can be utilized as an efficient drug in the treatment of ovarian cancer in humans.

Authors' contributions

All authors contributed and discussed in the analysis and results and commented on the manuscript. All authors read and approved the final manuscript.

Disclosure statement

No potential conflict of interest was reported by the authors.

Ethical approval

The study did not involve Human Participants and/or Animals.

Funding

Role and mechanism of nickel metabolism inhibitors in the treatment of ovarian cancer Project number: 2020-2017-074.

References

1. Ghashghaii A, Hashemnia M, Nikousefat Z, et al.Wound healing potential of methanolic extract of Scrophularia striata in rats. Pharm Sci. 2017;69:535–543.
2. Abdoli M, Sadrjavadi K, Arkan E, et al. In situ decorated Au NPs on pectin-modified Fe3O4 NPs as a novel magnetic nanocomposite (Fe3O4/Pectin/Au) for catalytic reduction of nitroarenes and investigation of its anti-human lung cancer activities. Int J Biol Macromol. 2020;163:2162–2171.
3. Mahdavi B, Paydarfard S, Zangeneh MM, et al. Assessment of antioxidant, cytotoxicity, antibacterial, antifungal, and cutaneous wound healing activities of green synthesized manganese nanoparticles using Ziziphora clinopodioides Lam leaves under in vitro and in vivo condition. Appl Organometal Chem. 2019;33:e5248.
4. Mahendran D, Kavi Kishor P, Geetha N, et al. Efficient antibacterial/biofilm, anti-cancer and photocatalytic potential of titanium dioxide nanocatalysts green synthesised using gloriosa superba rhizome extract. J Exp Nanosci. 2021;16(1):11–31.
5. Mirnezami SMS, Heydarinasab A, Akbarzadeh A, et al. Investigation of characterization and cytotoxic effect of PEGylated nanoliposomal containing melphalan on ovarian cancer: an in vitro study. J Exp Nanosci. 2021;16(1):102–116.
6. Venugopal N, Saiprakash P, Jayalakshmi M, et al. A study on the effect of nanosized tin oxide on the electrochemical performance of nanosized nickel hydroxide in alkali solution. J Exp Nanosci. 2013;8(5):684–693.
7. Sagadevan S, Vennila S, Muthukrishnan L, et al. Exploring the therapeutic potentials of phyto-mediated silver nanoparticles formed via calotropis procera (ait.) R. Br. root extract. J Exp Nanosci. 2020;15(1):217–231.
8. Hummers WS, Offeman RE. Preparation of graphitic oxide. J Am Chem Soc. 1958;80(6):1339–1339.
9. Aman S, Gupta UK, Singh D, et al. Herbal treatment for the ovarian cancer. SGVU J Pharmac Res Educ. 2018;3(2):325–329.
10. Liu J, Zangeneh A, Zangeneh MM, et al. Antioxidant, cytotoxicity, anti-human esophageal squamous cell carcinoma, anti-human caucasian esophageal carcinoma, anti-adenocarcinoma of the gastroesophageal junction, and anti-distal esophageal adenocarcinoma properties of gold nanoparticles green synthesized by Rhus coriaria L. fruit aqueous extract. J Exp Nanosci. 2020;15(1):202–216.
11. Rakotondramasy-Rabesiaka L, Havet J-L, Porte C, et al. Solid–liquid extraction of protopine from *fumaria officinalis* L.—experimental study and process optimization. Sep Purif Technol. 2008;59(3):253–261.,
12. Raafat KM, El-Zahaby SA. Niosomes of active fumaria officinalis phytochemicals: antidiabetic, anti-neuropathic, anti-inflammatory, and possible mechanisms of action. Chin Med. 2020;15:40.
13. Ognyanov M, Georgiev Y, Petkova N, et al. Isolation and characterization of pectic polysaccharide fraction from in vitro suspension culture of *fumaria officinalis* L. Int J Polymer Sci. 2018;2018:1–13.
14. Al-Snafi AE. Constituents and pharmacology of *Fumaria officinalis*-A review. IOSR J Pharm. 2020;10:17–25.
15. Rakotondramasy-Rabesiaka L, Havet J-L, Porte C, et al. Solid–liquid extraction of protopine from *fumaria officinalis* L.—analysis determination, kinetic reaction and model building. Sep Purif Technol. 2007;54(2):253–261.

16. Sturm S, Strasser E-M, Stuppner H. Quantification of *fumaria officinalis* isoquinoline alkaloids by nonaqueous capillary electrophoresis-electrospray ion trap mass spectrometry. J Chromatogr A. 2006;1112(1-2):331–338.
17. Paltinean R, Toiu A, Wauters J-N, et al. Phtochemical analysis of *Fumaria officinalis* L. (Fumariaceae). Farmacia. 2016;64:409–413.
18. Mahdavi B, Paydarfard S, Rezaei-Seresht E, et al. Green synthesis of NiONPs using Trigonella subenervis extract and its applications as a highly efficient electrochemical sensor, catalyst, and antibacterial agent. Appl Organomet Chem. 2021;35(8):e6264.
19. Shaneza A, et al. Herbal treatment for the ovarian cancer. SGVU J Pharma Res Educ. 2018;3(2): 325–329.
20. Arunachalam KD, et al. One-step green synthesis and characterization of leaf extract-mediated biocompatible silver and gold nanoparticles from memecylon umbellatum. Int J Nanomedicine. 2003;8: 1307–1315.
21. Zhang Y, Mahdavi B, Mohammadhosseini M, et al. Green synthesis of NiO nanoparticles using Calendula officinalis extract: chemical charactrization, antioxidant, cytotoxicity, and anti-esophageal carcinoma properties. Arabian J Chem. 2021;14(5):103105.
22. Iqbal J, Abbasi BA, Mahmood T, et al. Green synthesis and characterizations of nickel oxide nanoparticles using leaf extract of Rhamnus virgata and their potential biological applications. Appl Organometal Chem. 2019;33(8):e4950.
23. Mahdavi B, Saneei S, Qorbani M, et al. Ziziphora clinopodioides Lam leaves aqueous extract mediated synthesis of zinc nanoparticles and their antibacterial, antifungal, cytotoxicity, antioxidant, and cutaneous wound healing properties under in vitro and in vivo conditions. Appl Organometal Chem. 2019;33(11):e5164.
24. Baghayeri M, Mahdavi B, Hosseinpor-Mohsen Abadi Z, et al. Green synthesis of silver nanoparticles using water extract of salvia leriifolia: Antibacterial studies and applications as catalysts in the electrochemical detection of nitrite. Appl Organometal Chem. 2018;32(2):e4057.
25. Sharmila G, Thirumarimurugan M, Muthukumaran C. Green synthesis of ZnO nanoparticles using Tecoma castanifolia leaf extract: characterization and evaluation of its antioxidant, bactericidal and anticancer activities. Microchem J. 2019;145:578–587.
26. Nwanya AC, Ndipingwi MM, Ikpo CO, et al. Zea mays lea silk extract mediated synthesis of nickel oxide nanoparticles as positive electrode material for asymmetric supercabattery. J Alloys Compd. 2020;822:153581.
27. Baranwal K, Dwivedi LM, Singh V. Guar gum mediated synthesis of NiO nanoparticles: an efficient catalyst for reduction of nitroarenes with sodium borohydride. Int J Biol Macromol. 2018;120: 2431–2441.
28. Rameshthangam P, Chitra JP. Synergistic anticancer effect of green synthesized nickel nanoparticles and quercetin extracted from Ocimum sanctum leaf extract. J Mater Sci Technol. 2018;34(3): 508–522.
29. Ibraheem F, Aziz MH, Fatima M, et al. In vitro cytotoxicity, MMP and ROS activity of green synthesized nickel oxide nanoparticles using extract of Terminalia chebula against MCF-7 cells. Mater Lett. 2019;234:129–133.
30. Chen M, Zhang Y, Huang B, et al. Evaluation of the antitumor activity by Ni nanoparticles with verbascoside. J Nanomater. 2013;2013:1–6.
31. Al-Snafi A. The chemical constituents and pharmacological effects of calendula officinalis-A review. Indian J Pharma Sci Res. 2015;5:172–185.
32. Ezhilarasi AA, Vijaya JJ, Kaviyarasu K, et al. Green synthesis of NiO nanoparticles using Moringa oleifera extract and their biomedical applications: Cytotoxicity effect of nanoparticles against HT-29 cancer cells. J Photochem Photobiol B. 2016;164:352–360.
33. Petruczynik A, Plech T, Tuzimski T, et al. Determination of selected isoquinoline alkaloids from *Mahonia aquifolia*; *Meconopsis cambrica*; *Corydalis lutea*; *Dicentra spectabilis*; *Fumaria officinalis*; *Macleaya cordata* extracts by HPLC-DAD and comparison of their cytotoxic activity. Toxins. 2019; 11:575.
34. (a) Veisi H, Tamoradi T, Karmakar B, Mohammadi, et al. In situ biogenic synthesis of Pd nanoparticles over reduced graphene oxide by using a plant extract (Thymbra spicata) and its catalytic evaluation towards cyanation of aryl halides. Mater Sci Eng C Mater Biol Appl. 2018;104:109919.,
35. You C, Han C, Wang X, et al. The progress of silver nanoparticles in the antibacterial mechanism, clinical application and cytotoxicity. Mol Biol Rep. 2012;39(9):9193–9201..
36. Mao B-H, Tsai J-C, Chen C-W, et al. Mechanisms of silver nanoparticle-induced toxicity and important role of autophagy. Nanotoxicology. 2016;10(8):1021–1040.

37. Namvar F, Rahman HS, Mohamad R, et al. Cytotoxic effect of magnetic iron oxide nanoparticles synthesized via seaweed aqueous extract. Int J Nanomedicine. 2014;19:2479–2488.
38. Sankar R, Maheswari R, Karthik S, et al. Anticancer activity of Ficus religiosa engineered copper oxide nanoparticles. Mater Sci Eng C Mater Biol Appl. 2014;44:234–239.
39. Katata-Seru L, Moremedi T, Aremu OS, et al. Green synthesis of iron nanoparticles using Moringa oleifera extracts and their applications: Removal of nitrate from water and antibacterial activity against Escherichia coli. J Mol Liq. 2018;256:296–304.
40. Sangami S, Manu M. Synthesis of green iron nanoparticles using laterite and their application as a fenton-like catalyst for the degradation of herbicide Ametryn in water. Environ Technol Innov. 2017;8:150–163.
41. Beheshtkhoo N, Kouhbanani MAJ, Savardashtaki A, et al. Green synthesis of iron oxide nanoparticles by aqueous leaf extract of Daphne mezereum as a novel dye removing material. Appl Phys A. 2018;124:363–369.
42. Radini IA, Hasan N, Malik MA, et al. Biosynthesis of iron nanoparticles using Trigonella foenum-graecum seed extract for photocatalytic methyl orange dye degradation and antibacterial applications. J Photochem Photobiol B. 2018;183:154–163.